doi:10.1017/S1431927615013288

A Parallel Radial Mirror Energy Analyzer Attachment for the Scanning Electron Microscope

Kang Hao Cheong, Weiding Han, Anjam Khursheed and Karuppiah Nelliyan

National University of Singapore, Department of Electrical and Computer Engineering, 4 Engineering Drive 3, Singapore 117576, Singapore, g0800484@nus.edu.sg

This paper aims to further develop the Parallel Radial Mirror Analyzer (PRMA) as an attachment for the Scanning Electron Microscope (SEM), to be used as a wide-band multi-channel analyzer attachment for carrying out Auger Electron Spectroscopy (AES) [1]. The PRMA has a predicted transmittance of over two orders of magnitude higher and an energy resolution advantage of around 6 times better than the Hyperbolic Field Analyzer (HFA) [2], the electric field multi-channel analyzer design that had previously been proposed for AES in the SEM. These advantages come from its fully rotationally symmetric detection plane (2π collection in the azimuthal direction) and second-order focusing properties for all electrons that are detected. However, in comparison with the HFA, the PRMA is a much more complicated analyzer design due to the requirement of 12 electrodes and electrons travelling through an exit grid. There is also the challenge in finding a curvilinear shaped position sensitive detector.

Khursheed et al. arrived at the PRMA design by carrying out direct ray tracing of electrons with the two-dimensional commercial Lorentz 2EM software [3]. In this work, a Damped-Least Squares (DLS) module was combined with the Lorentz software in order to modify the PRMA design. The DLS method of optimisation is first applied for extending the analyzer working distance to 7 mm without significantly compromising the relative energy resolution. The parameters to be adjusted for the PRMA are twelve electrode voltages, while the parameter to be minimized is the average output relative energy resolution (which includes 30 different energies). Optimisation of electrode voltages was carried out with the constraint of the detection plane being flat (lying on a horizontal plane). If the analyzer working distance is extended beyond 8 mm, the average relative energy resolution is predicted to grow by around a factor of two (over 0.30%). For an analyzer working distance of 7 mm, measured radially from the optical axis and axially from the specimen surface (with the optimal polar emission angle for the central ray found to be 24.2º), simulation results predict that the average relative energy resolution on a horizontal detector plane will grow from 0.14% (corresponding to the current working distance of 3.5 mm) to 0.23%, indicating that the working distance of the PRMA can be doubled without significantly degrading its average relative energy resolution. Figure 1a shows the simulated trajectory paths through the PRMA design for an analyzer working distance of 7 mm after applying the DLS optimization method. Equipotential lines are plot from -176 to -2464 V in uniform steps of -176 V. At each energy, seven trajectories are plot evenly between -3° and 3° around a 24.2º polar entrance angle. Figure 1b shows the analyzer electrode voltages for the modified design.

Figure 2a shows ray tracing around the output focal plane at 1% above and below the selected energies of 600, 2000, 3500 and 5000 eV for an angular spread of $\pm 3^\circ$ in uniform steps of 1º for the modified PRMA design with an analyzer working distance of 7 mm. They indicate that the predicted energy resolution (corresponding to the half-width of the central ray) is around 0.2% for a wide range of energies. Figure 2b shows that the simulated focusing properties of the analyzer design are of second-order for three selected energies (third-order aberration dependence). Similar trace-width diagrams like

these were obtained for other energies, confirming that second-order focusing is predicted over the entire electron energy range of detection. The simulation results in Figure 2b are similar to the ones in the original PRMA design [1], indicating that second-order focusing properties are retained despite it having a larger analyzer working distance.

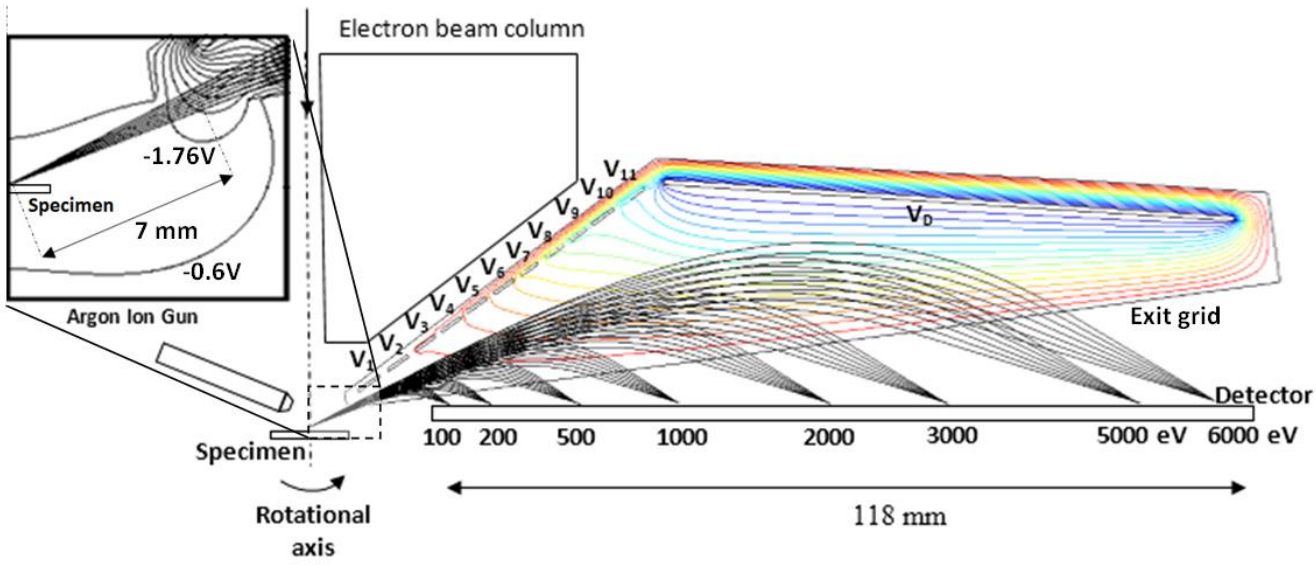

(a)

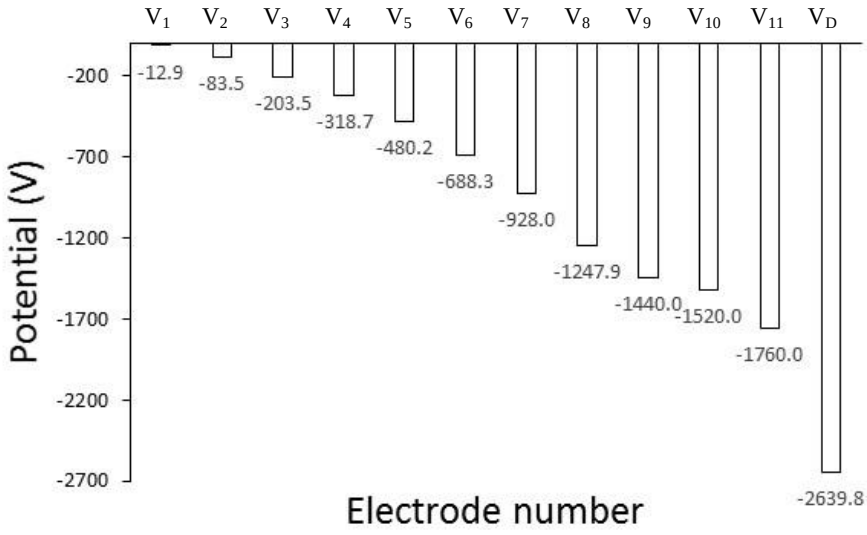

(b)

Figure 1. Modified PRMA design for an analyser working distance of 7 mm: (a) Direct ray tracing of seven trajectories plotted evenly between −3◦ and 3◦ around a 24.2º polar entrance angle. Equipotential lines plot from -176 to -2464 V in uniform steps of -176 V are also indicated; (b) Electrode potentials.

Figure 3 shows a comparison of the simulated relative energy resolution for the PRMA design in comparison with the HFA design for a polar angular spread of ± 3°. The average relative energy resolution for the HFA and PRMA design (with a working distance of 7 mm) is 1.528% and 0.23%

respectively on the detector plane across the entire electron energy range of 100 eV to 5000 eV. For most of the energy range, the PRMA design has an energy resolution that is around 7.5 times better than the HFA. The poorer energy resolution predicted for low energies (< 200 eV) is caused by the analyzer open entrance, where fringe fields (indicated in Figure 1) are created. While simulations predict that a grid placed at the entrance improves the relative energy resolution by a factor of 2 for the lower electron energy range (< 200 eV), an entrance grid has the disadvantages of lowering the overall transmission and is difficult to fabricate. A better proposal would be to extend the upper range of the detection range. Preliminary simulation results indicate that a modified analyzer design can in principle be made for an energy range extended up to 8,000 eV, however, more simulations are required to investigate the quality of the analyzer's focussing properties at the high part of the extended range.

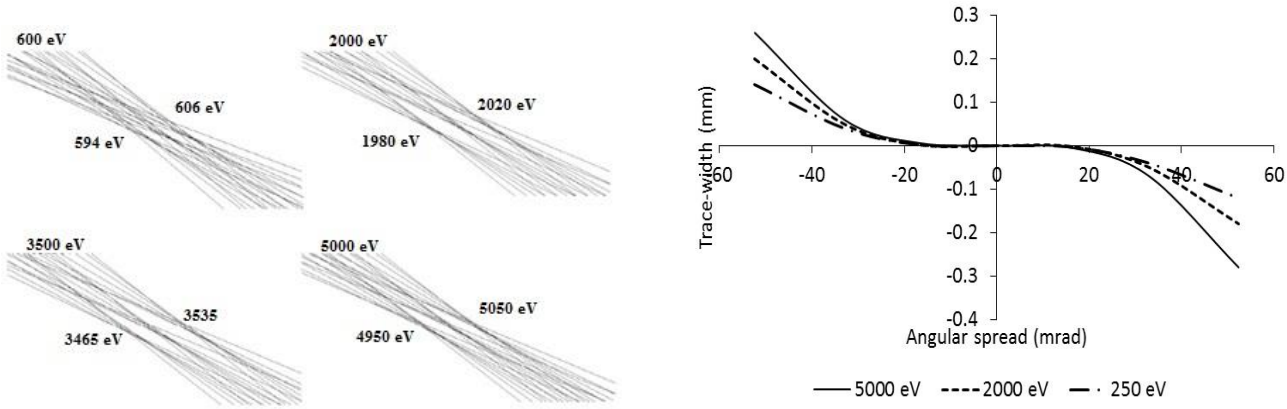

(a) (b)

Figure 2. Simulated characteristics on the focal plane at selected energies of the PRMA design, for an angular spread of ±3◦ in uniform steps of 1º: (a) Trajectory paths with energies at ±1% below and above the central energies of 600, 2000, 3500 and 5000 eV; (b) Trace-width as a function of polar angular spread on the Gaussian focal plane at selected energies. The polar angular spread ranges from −3º to +3º.

Several designs for the exit grid were analyzed by the use of the Lorentz 3EM program [3]. Each grid layout is assessed in terms of its adverse effect on the energy resolution for 90% transparency. Figure 4 shows 3 possible exit grid designs (not drawn to scale): (a) a square grid design, (b) a radial slot design and (c) a layered radial slot design.

The square grid design is the one that is most readily available commercially. However, one limitation of the square grid design is that it is not rotationally symmetric and causes greater scattering of electrons. The radial slot grid is designed to reduce scattering, however, a radial slot design suffers from the limitation that the separation between each wire increases with radius. As the separation of the wires increases, leakage fields become larger and degrade the focusing properties of the analyzer. The layered slot grid is designed to maintain a similar separation distance between wires as a function of radius, and thereby reduces fringe field effects. Simulation results shown in Figure 5 predict that the fringe field effects due to the square grid is likely to produce a relative energy resolution that is considerably worse than those obtained by the other two grid layouts in the lower half of the energy range. The average relative energy resolution for the square grid, radial slot and layered radial slot designs are 0.36%, 0.27% and 0.25% respectively (for 90% grid transparency). These simulation results indicate that the

radial slot and layered radial slot grids are the better ones to use. These simulation results also indicate that the introduction of an appropriate exit grid design is not going to significantly degrade the focusing properties of the analyzer for most the energy range, and it is the focusing properties of the analyzer in the lower energy region that will be affected the most. Since the relative energy resolution of the analyzer is comparatively worse in the lower energy range (< 200 eV), this is another reason for moving the energy detection range to a higher one, say from 200 eV to 8 KeV.

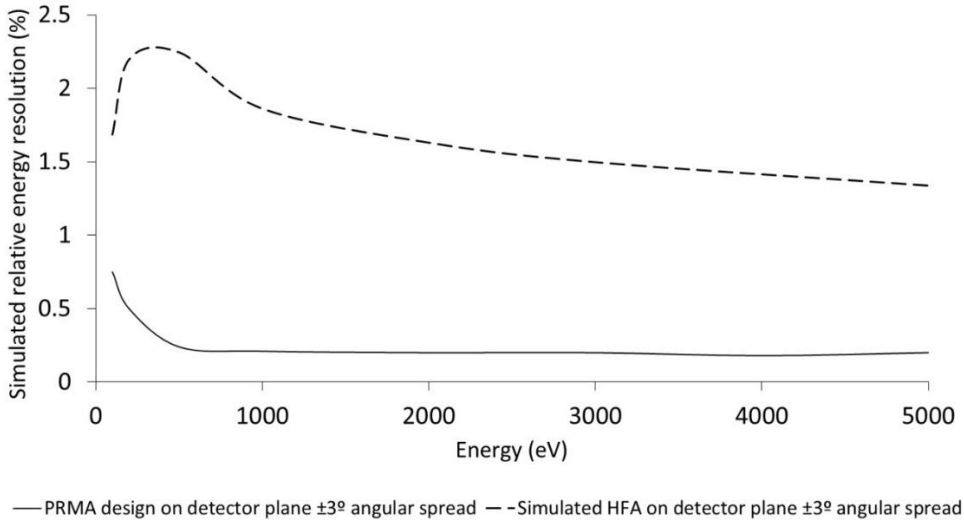

Figure 3. Simulated relative energy resolution for the PRMA design as a function of energy in comparison with the HFA for a polar angular spread of ± 3°.

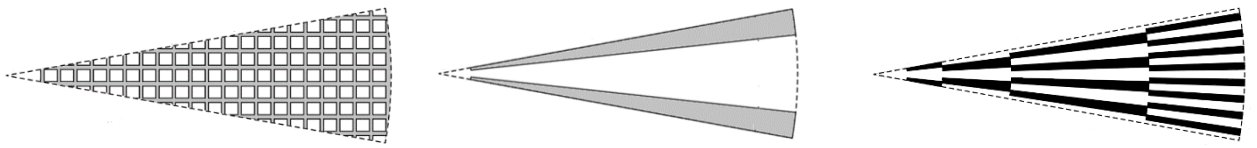

(a) (b) (c)

Figure 4. Schematic diagram of 3 possible exit grids design (not drawn to scale): (a) Square grid design; (b) Radial slot design; (c) Layered radial slot design.

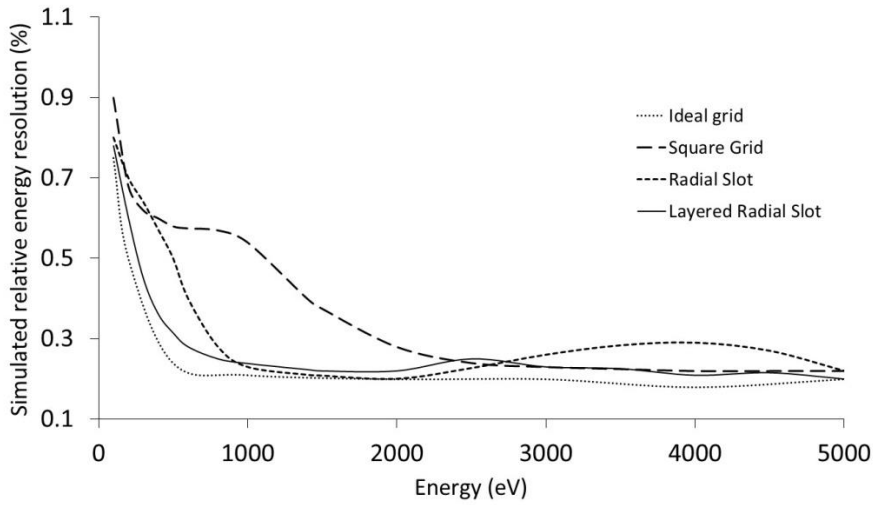

Figure 5. Simulated energy resolution of the PRMA as a function of energy for different exit grid designs.

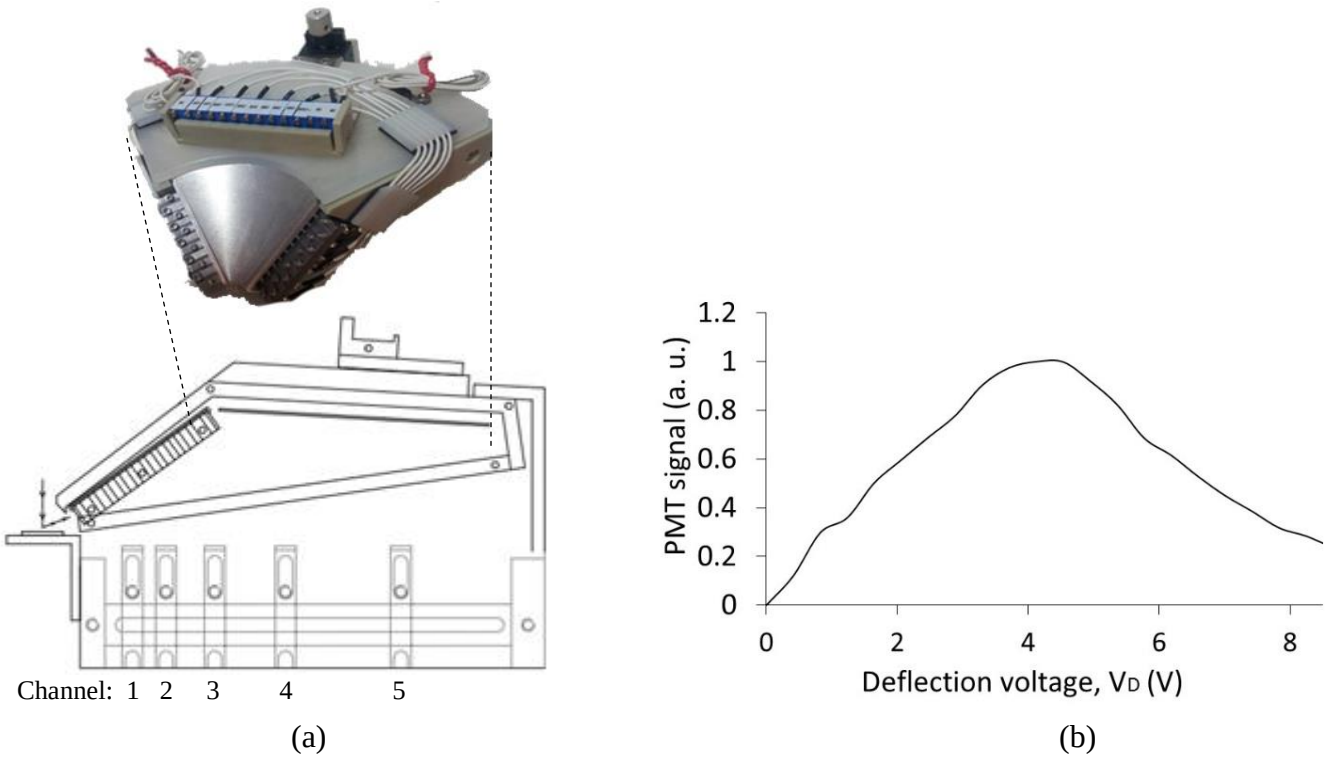

Figure 6. PRMA prototype designed for the SEM and a schematic of its detection system. (a) Photograph of the PRMA prototype with energy channel 1 to 5; (b) Experimental analyzer signals obtained in a SEM.

A PRMA prototype was designed to fit into the specimen chamber of a Philips XL30 ESEM-FEG, but it can also be used for a standalone AES system. The prototype was made in the form of a sector module extending 110º in the azimuthal direction, although, only a small fraction of the azimuthal angular range was used in practice due to detector constraints. A schematic of the prototype and its array of detectors

are shown in Figure 6a, together with a photograph of the PRMA prototype. The primary beam of the SEM was focused onto the surface of a Silicon (Si) wafer specimen coated with Silver (Ag) of 500 nm thickness. The deflection voltage was ramped in steps of 0.5V and each point had a primary beam dwell time of ~120 ms. The strength of all other analyzer electrode voltages are scaled to V_D. At a primary beam energy of 5 keV, the beam current was measured to be 150 pA. Figure 6b shows an initial experimental SE spectrum at channel 5 of the PRMA operated as a sequential spectrometer inside the SEM, confirming that the prototype can function as a conventional SE spectrometer. The PRMA was also placed inside a dedicated vacuum chamber with a field emission gun. A single PMT with scintillator unit was successively placed at three different energy channels (channel 1, 3 and 5 as indicated on Figure 6a). The PMT signals were then recorded as a function of V_D and are shown in Figure 7a. The pass energies for channels 1, 3, and 5 are 0.0348, 0.139 and 0.556 times V_D respectively, derived by simulation. Figure 7b shows the transformed SE energy spectrum from each channel. These preliminary experimental results show that the analyzer optics operates as predicted by simulation, and is approximately the same across the detected energy range. The SE peak corresponding to silver can be observed in both Figures 6b and 7b. Future work will, widen the azimuthal angular range of detection, measure the energy resolution of the PRMA experimentally, and use it to acquire Auger spectra [4].

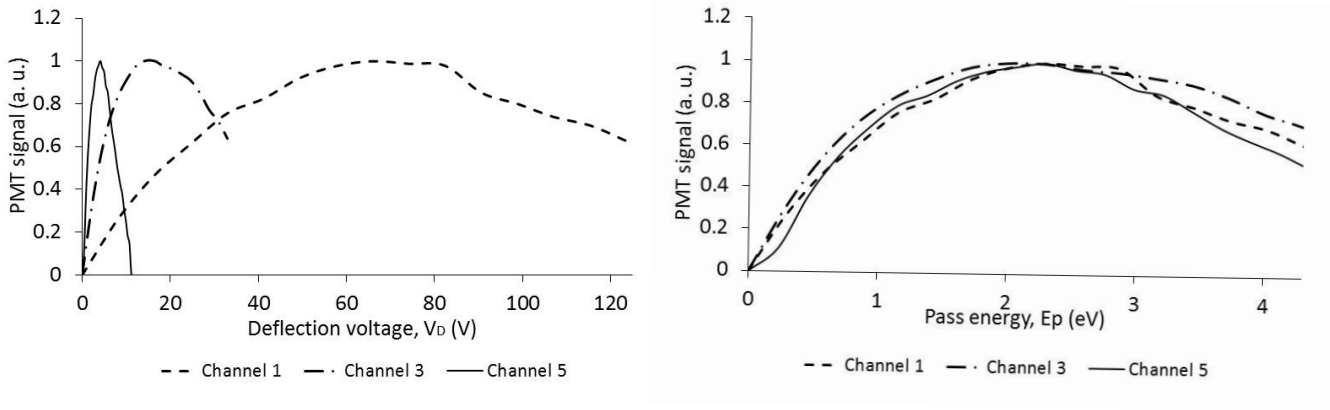

Figure 7. Preliminary experimental results from 3 different representative channels along the dispersion plane. Left: PMT signal as a function of deflection voltage, V_D (V); right: PMT signal as a function of pass energy, E_p (eV).

References

[1] A Khursheed, HQ Hoang and A Srinivasan, J. Electron. Spectrosc. **184** (2012), p. 525.
[2] M Jacka *et al*, Rev. Sci. Instrum. **70** (1999), p. 2282.
[3] Lorentz-2EM/3EM, Integrated Engineering Software Inc., Canada, 2011.
[4] The authors acknowledge funding under the Singapore Government MOE 2011-T2-2-108.